

(18). This constriction may provoke coronary vasospasm which could trigger an acute ischemic crisis. Thus, PGI<sub>2</sub> may be useful in the prevention of secondary ischemic episodes once an initial ischemic event occurs in the heart.

ALLAN M. LEFER

MARTIN L. OGLETREE

Department of Physiology,  
Thomas Jefferson University,  
Philadelphia, Pennsylvania 19107

J. BRYAN SMITH

MELVIN J. SILVER

Cardeza Foundation and  
Department of Pharmacology,  
Thomas Jefferson University

KYRIACOS C. NICOLAOU

WILLIAM E. BARNETTE

GREGORY P. GASIC

Chemistry Department, University of  
Pennsylvania, Philadelphia 19174

#### References and Notes

1. S. Moncada, R. Gryglewski, S. Bunting, J. R. Vane, *Nature (London)* **263**, 663 (1976); S. Bunting, R. Gryglewski, S. Moncada, J. R. Vane, *Prostaglandins* **12**, 897 (1976); S. Moncada, R. J. Gryglewski, S. Bunting, J. R. Vane, *ibid.*, p. 715; R. A. Johnson, D. R. Morton, J. H. Kinner, R. R. Gorman, J. C. McGuire, F. F. Sun, N. Whittaker, S. Bunting, J. Salmon, S. Moncada, J. R. Vane, *ibid.*, p. 915.
2. M. L. Ogletree and A. M. Lefer, *Circ. Res.* **42**, 218 (1978); T. Takano, J. K. Vyden, H. B. Rose, E. Corday, H. J. C. Swan, *Am J. Cardiol.* **39**, 297 (1977).
3. K. C. Nicolaou, W. E. Barnette, G. P. Gasic, R. L. Magolda, W. J. Sipio, M. J. Silver, J. B. Smith, C. M. Ingerman, *Lancet* **1977-I**, 1058 (1977). This methodology has been successfully extended to the synthesis of other more stable PGI<sub>2</sub> derivatives [K. C. Nicolaou, W. E. Barnette, G. P. Gasic, R. L. Magolda, *J. Am. Chem. Soc.* **99**, 7736 (1977)].
4. E. E. Selkurt, *Physiology* (Little, Brown, Boston, ed. 4, 1976), p. 419; A. M. Lefer and J. A. Spath, Jr., in *Cardiovascular Pharmacology*, M. J. Antonaccio, Ed. (Raven, New York, 1977), p. 377.
5. M. L. Ogletree and A. M. Lefer, *Fed. Proc. Fed. Am. Soc. Exp. Biol.* **36**, 986 (1977).
6. A. M. Lefer, *J. Pharmacol. Exp. Ther.* **151**, 294 (1966). The composition of the modified Krebs-Henseleit solution in millimoles per liter was

NaCl, 118; KCl, 4.75; CaCl<sub>2</sub> · H<sub>2</sub>O, 2.54; KH<sub>2</sub>PO<sub>4</sub>, 1.19; MgSO<sub>4</sub> · 7H<sub>2</sub>O, 1.19; NaHCO<sub>3</sub>, 12.50; and glucose, 10.0.

7. N. Toda, H. Usui, K. Sakae, *Jpn. J. Pharmacol.* **25**, 487 (1975); R. Boroyan, *Acta Biol. Med. Ger.* **35**, 1083 (1976); S. Kalsner, *Can. J. Physiol. Pharmacol.* **53**, 560 (1975).
8. R. M. Berne, *Physiol. Rev.* **44**, 1 (1964).
9. A. M. Lefer, R. Cowgill, F. F. Marshall, L. M. Hall, E. D. Brand, *Am. J. Physiol.* **213**, 492 (1967); A. M. Lefer, *Fed. Proc. Fed. Am. Soc. Exp. Biol.* **29**, 1836 (1970); L. J. Greene, R. Shapanka, T. M. Glenn, A. M. Lefer, *Biochim. Biophys. Acta* **491**, 275 (1977). Myocardial depressant factor has been identified as a tetrapeptide having a molecular weight of 500.
10. J. T. Flynn, G. A. Bridenbaugh, A. M. Lefer, *Am. J. Physiol.* **230**, 684 (1976); T. M. Glenn and A. M. Lefer, *Circ. Res.* **27**, 783 (1970).
11. Cathepsin D activity was assayed according to the method of M. L. Anson [*J. Gen. Physiol.* **20**, 565 (1936)], bovine hemoglobin being used as substrate. One unit of cathepsin D activity is equivalent to 1 mEq of tyrosine release × 10<sup>-4</sup> per milliliter per hour at 37°C. β-Glucuronidase activity was assayed according to the method of P. Talalay, W. Fishman, and C. Huggins [*J. Biol. Chem.* **166**, 757 (1946)], phenolphthalein glucuronide being used as substrate. One unit of β-glucuronidase activity is equivalent to 1 μg of phenolphthalein × 10<sup>-2</sup> released per milliliter per hour at 37°C.
12. G. T. Rafo, S. L. Wangenstein, T. M. Glenn, A. M. Lefer, *Eur. J. Pharmacol.* **24**, 86 (1973).
13. G. V. R. Born, *Nature (London)* **194**, 927 (1962).
14. V. Ferraris, J. B. Smith, M. J. Silver, *Thromb. Diath. Haemorrh.* **38**, 20 (1977); R. R. Gorman, S. Bunting, O. V. Miller, *Prostaglandins* **13**, 377 (1977); J. E. Tateos, S. Moncada, J. R. Vane, *ibid.*, p. 389; C. Malmsten, E. Granström, B. Samuelsson, *Biochem. Biophys. Res. Commun.* **68**, 569 (1976).
15. E. Braunwald, in *Pathophysiology and Therapeutics of Myocardial Ischemia*, A. M. Lefer, G. J. Kellier, M. J. Rovetto, Eds. (Spectrum, New York, 1977), p. 265; P. R. Maroko and E. Braunwald, *Ann. Intern. Med.* **79**, 720 (1973).
16. M. A. Ricciutti, *Am. J. Cardiol.* **30**, 492 (1972); *ibid.*, p. 498; J. A. Spath, Jr., and A. M. Lefer, *Circ. Res.* **35**, 44 (1974); G. Weissmann, S. Hoffstein, D. Gennaro, A. C. Fox, in *Pathophysiology and Therapeutics of Myocardial Ischemia*, A. M. Lefer, G. J. Kellier, M. J. Rovetto, Eds. (Spectrum, New York, 1977), p. 367.
17. T. M. Glenn, A. M. Lefer, A. C. Beardsley, W. W. Ferguson, A. M. Lopez-Rasi, T. S. Serate, J. R. Morris, S. L. Wangenstein, *Ann. Surg.* **176**, 120 (1972); J. A. Spath, Jr., E. A. Reed, A. M. Lefer, *ibid.* **181**, 813 (1975).
18. E. F. Ellis, O. Olez, L. J. Roberts, II, N. A. Payne, B. J. Sweetman, A. S. Nies, J. A. Oates, *Science* **193**, 1135 (1976); P. A. Needleman, P. S. Kulkarni, A. Raz, *ibid.* **195**, 409 (1977).
19. We thank M. Gaffney and C. M. Ingerman for technical assistance.

26 September 1977; revised 28 December 1977

## Size and Shape of the Lateral Intercellular Spaces in a Living Epithelium

**Abstract.** *The lateral intercellular spaces of Necturus gallbladder epithelium were seen and measured while the living tissue was perfused in a new chamber. The compliance of the lateral cell membranes was calculated from the measured pressure-volume characteristics of the lateral intercellular spaces.*

The lateral intercellular spaces of fluid-transporting epithelia have been assigned a major role in the transepithelial movement of water. On the basis of electron micrographs of rabbit gallbladder, it was concluded that the size of the lateral spaces was directly related to the rate of isotonic fluid transport by the gallbladder and that the interspaces represent the final common path for transported fluid (1). Several aspects of these results have been called into question. It has been

suggested that the dimensions of the lateral spaces are such that current mathematical models fail to predict an isotonic absorbate (2). Fredericksen and Rostgaard (3) even questioned the existence of dilated lateral intercellular spaces in living preparations and suggested that the fixation and embedding procedures preparative to electron microscopy produced artificially dilated spaces because of cell shrinkage. Other authors (4) reported that fixation procedures may alter

intercellular space geometry, making the accuracy of morphometric data questionable.

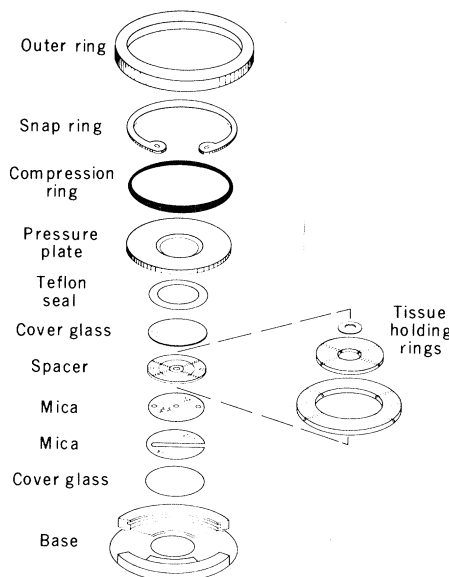
The conclusions of many investigators about the role of the lateral spaces are heavily dependent on the accuracy of measurements of the spaces in electron micrographs. Since there is controversy about the relevance of intercellular dimensions in fixed preparations to the living tissue, we developed a method for light microscopic observation of the spaces in a living, flat epithelium. This system makes it possible to continuously measure the width or cross-sectional area of the lateral intercellular spaces at any distance between the tight junction and the basement membrane. Simultaneously, we can measure the epithelial electrical resistance, pass current across the epithelium, vary and measure the hydrostatic pressure across the epithelium, and rapidly alter the composition of the fluids bathing either surface of the epithelium. Thus it is possible to perform most of the experiments currently utilized for studying epithelia while monitoring the size and shape of the intercellular spaces. *Necturus* gallbladder was chosen for the initial experiments because of its relatively large cell size (15 to 25 μm in diameter) (5).

The chamber for the gallbladder, shown in an exploded view in Fig. 1, is a miniature Ussing chamber (6) whose dimensions are chosen to satisfy the optical requirements of the microscope lens system. The overall chamber thickness is 1.1 mm and the tissue is within 75 μm of the inner surface of the bottom cover glass. The chamber was modified from a Dvorak-Stotler tissue culture chamber (7). The tissue is held mucosal side downward between concentric rings that are placed inside a plastic spacer. The bottom of the spacer is composed of two laminated sheets of mica and the bottom cover glass (Fig. 1). The channel in the lower mica forms the mucosal bath (8). The serosal bath is formed by fluid above the smallest tissue-holding ring. Before assembly, the topmost mica surface was painted lightly with liquid Sylgard 184 (Dow Chemical Co., Midland, Michigan) to achieve an electrical seal of the tissue to the mica around the center hole. The size of the center hole in the uppermost mica sheet determines the area of tissue exposed to the mucosal bath. We tried several sizes, ranging in diameter from 75 μm to 1.5 mm. The optimum size was a 1.5-mm-diameter hole, determined by the electrical properties of the tissue and mechanical considerations. Thus the exposed tissue has an area of 1.8 × 10<sup>-2</sup> cm<sup>2</sup>.

The chamber is placed on the stage of an inverted microscope (Diavert; E. Leitz, Rockleigh, New Jersey), as shown in Fig. 2. The microscope is used in the direct illumination mode and is equipped with several special optical features (9), which may be briefly summarized as follows. The preparation is illuminated by a stabilized light source through a high-magnification objective lens-condenser, and the image is formed by an oil-immersion objective lens. When the condenser is properly positioned, the tissue is illuminated with a circle of light approximately  $75 \mu\text{m}$  in diameter. Since the optical system has an effective numerical aperture of 0.95, a shallow depth of focus is achieved and the tissue may be optically sectioned in approximately  $1\text{-}\mu\text{m}$  thicknesses. The image is split and 10 percent of the light is diverted to an image-intensified television camera; the remaining 90 percent goes to a photomultiplier tube (EMI 9844B phototube with S-11 cathode) after passing through a slit of variable dimensions. The measuring slit of the photometer is positioned over the lateral intercellular space of interest. The position of the slit and the focus are constantly monitored with the television system during measurements.

When the measuring slit of the photometer is placed over an interspace and the microscope is focused from the surface of the cells through the tissue to the basement membrane, the current output of the photometer is observed to vary. Serial measurements of the width of a lateral intercellular space at each focal depth were compared to the photomultiplier readings at each depth. The result is shown in Fig. 3. The width of interspaces with regular geometry was determined by directly reading a calibrated graticule in the television image. The accuracy of the width measurements is  $0.15 \mu\text{m}$ . Although there is no readily predictable theoretical relationship between lateral interspace dimensions and light transmission, we observed that the phototube current was a linear function of the cross-sectional area of the space in the focal plane. In all cases linear regression of phototube current on interspace width (or cross-sectional area for irregularly shaped spaces) yielded a correlation coefficient of .94 or larger.

*Necturus* gallbladder in the chamber exhibited electrical and selectivity properties comparable to those previously reported in larger chambers. Tissue resistance in chloride Ringer solution, measured by use of a voltage clamp with a triangular wave command (1 Hz), averaged  $330 \pm 29 \text{ ohm-cm}^2$  [mean  $\pm$  standard error (S.E.),  $N = 11$ ], comparable



to the value  $307 \text{ ohm-cm}^2$  previously reported (10). In sulfate Ringer solution the resistance was  $500 \pm 96 \text{ ohm-cm}^2$  (mean  $\pm$  S.E.,  $N = 6$ ), in agreement with a recent report (11). When the mucosal NaCl was totally replaced by tetramethylammonium chloride in six gallbladders, an average bionic potential of  $29 \pm 4 \text{ mV}$  developed (mucosa positive), consistent with the  $\text{Na}^+$  selectivity observed by several investigators (10). Tissue integrity, as assessed by electrical parameters and appearance, was well maintained for  $\sim 7$  hours. The mucosal and serosal baths were constantly perfused; when perfusion of the serosal bath was stopped for periods of more than 15 min-

utes the preparation deteriorated. The mucosal bath volume was approximately  $1.85 \mu\text{l}$  and was typically changed about ten times per minute. The serosal bath volume was approximately  $6 \mu\text{l}$  and was changed about five or six times per minute.

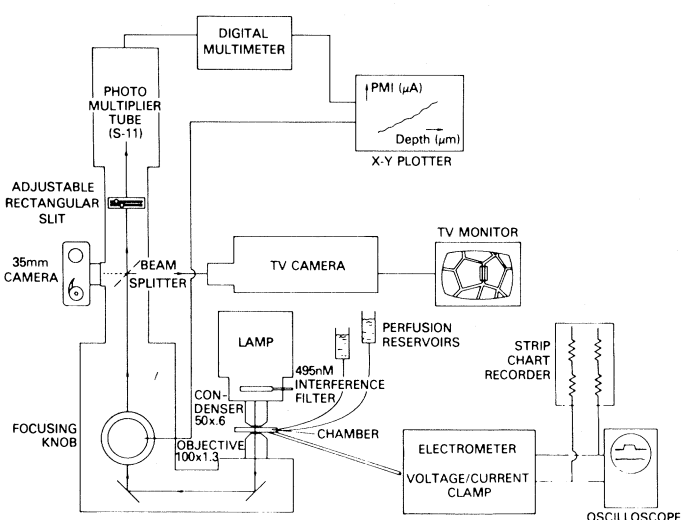
The top cover glass is held in place by silicone grease. The pressure plate, compression ring, and outer ring serve to hold the chamber securely to the base, which fits onto the microscope stage. The mica disks are  $25 \mu\text{m}$  (top) and  $50 \mu\text{m}$  (bottom) thick; the center hole in the top mica is  $1.5 \text{ mm}$  in diameter and determines the area of tissue exposed to the mucosal bath.

The outer and intermediate spacer rings have four holes drilled through their edges. Serosal bath fluid flows through two needles (not shown for clarity) pushed through two of these holes. These needles serve to deliver and remove fluid from the small region overlying the center ring. The two other holes are used for serosal voltage electrode and pressure transducer needles.

The top cover glass is held in place by silicone grease. The pressure plate, compression ring, and outer ring serve to hold the chamber securely to the base, which fits onto the microscope stage. The mica disks are  $25 \mu\text{m}$  (top) and  $50 \mu\text{m}$  (bottom) thick; the center hole in the top mica is  $1.5 \text{ mm}$  in diameter and determines the area of tissue exposed to the mucosal bath.

utes the preparation deteriorated. The mucosal bath volume was approximately  $1.85 \mu\text{l}$  and was typically changed about ten times per minute. The serosal bath volume was approximately  $6 \mu\text{l}$  and was changed about five or six times per minute.

The dimensions of the lateral intercellular spaces under conditions of normal fluid transport are critically important parameters in several mathematical models of isotonic fluid transport (12). We therefore determined the characteristic shape of the lateral spaces during fluid transport, when the mucosal and serosal bathing solutions were *Necturus* NaCl Ringer solution (13). A narrow rec-



of the photometer is observed to vary. Serial measurements of the width of a lateral intercellular space at each focal depth were compared to the photomultiplier readings at each depth. The result is shown in Fig. 3. The width of interspaces with regular geometry was determined by directly reading a calibrated graticule in the television image. The accuracy of the width measurements is  $0.15 \mu\text{m}$ . Although there is no readily predictable theoretical relationship between lateral interspace dimensions and light transmission, we observed that the phototube current was a linear function of the cross-sectional area of the space in the focal plane. In all cases linear regression of phototube current on interspace width (or cross-sectional area for irregularly shaped spaces) yielded a correlation coefficient of .94 or larger.

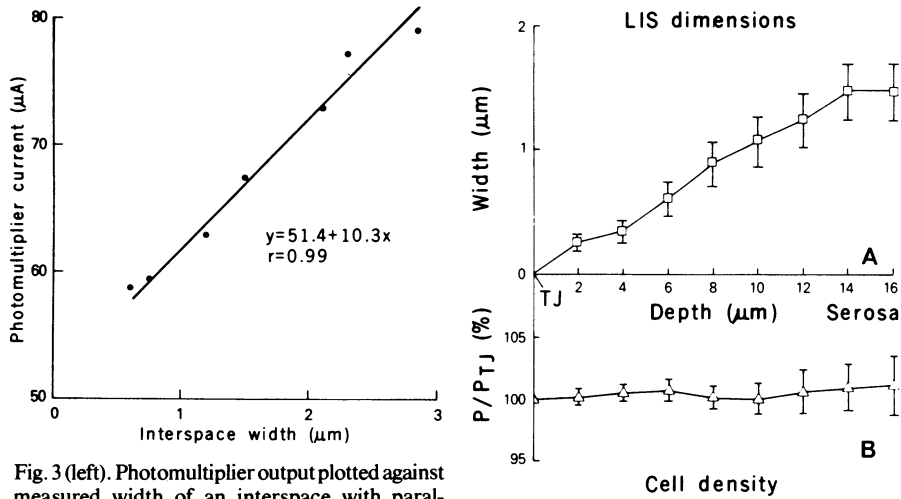


Fig. 3 (left). Photomultiplier output plotted against measured width of an interspace with parallel walls. Each point represents the record of light output and width for the same interspace at different depths of focus. The line is fitted by the method of least squares. Fig. 4 (right). (A) Dimensions and profile of the average lateral intercellular space (LIS) of *Necturus* gallbladder. The interspace depth of 16  $\mu\text{m}$  is a mean value ( $16 \pm 0.47 \mu\text{m}$ ,  $N = 23$ ) of the distance from the tight junction (TJ) to the serosal base of the cell. (B) Light transmission by the cells adjacent to the measured space;  $P/P_{TJ}$  is the percentage light transmission at any depth relative to that at the level of the tight junction. (A and B) Points show means  $\pm$  S.E.

tangular measuring slit was scanned from one cell across the interspace to the adjacent cell at 2- $\mu\text{m}$  intervals of depth from the tight junction to the base of the cells. Table 1 and Fig. 4 give the mean width of 23 spaces and the light transmission of their adjacent cells ( $N = 37$ ). The narrowest space width that could be detected was 0.30  $\mu\text{m}$ , which is near the limit of resolution of our optical system. The lateral space normally exhibited a very narrow region for 4 to 6  $\mu\text{m}$  beneath the tight junction and then a gradual increase in width as a function of depth. The width of the interspace was not uniform around the cell (14). Small dilations or "lakes" of fluid were frequently observed (Fig. 5), particularly at the junction of three cells. The formation of such local expansions of the interspace probably resulted from cell-to-cell coupling by desmosomes or interdigitations of lateral membranes of adjacent cells

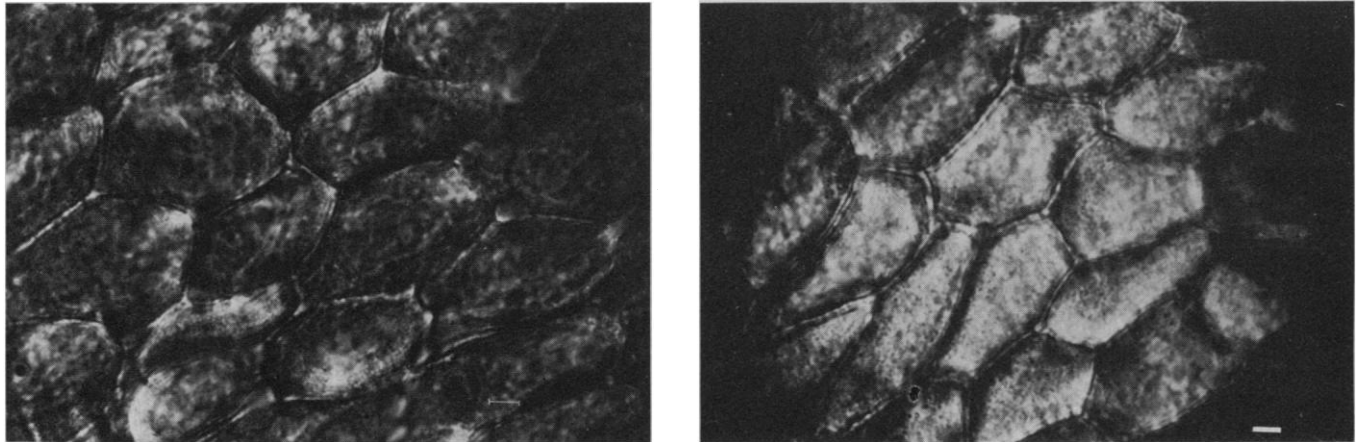


Fig. 5 (left). *Necturus* gallbladder bathed in chloride Ringer solution in the absence of a hydrostatic pressure gradient. The focus depth is 14  $\mu\text{m}$  below the tight junction. Note the narrow but discernible interspaces with expanded regions at the junction of three adjacent cells. Scale bar, 5  $\mu\text{m}$ . Fig. 6 (right). *Necturus* gallbladder, 15 cm-H<sub>2</sub>O hydrostatic pressure gradient (serosa > mucosa), bathed in chloride Ringer solution. The focus depth is 10  $\mu\text{m}$  below the tight junction. Note the regular banded appearance of interspace due to interdigitations or folds of adjacent lateral cell membranes. Scale bar, 5  $\mu\text{m}$ .

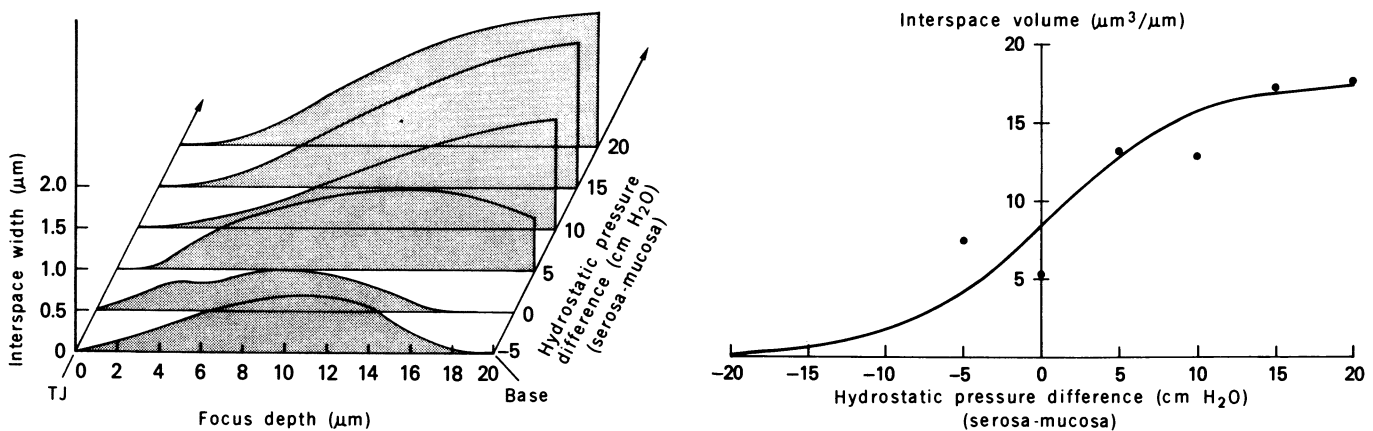


Fig. 7 (left). Record of the dimensions of one interspace at different hydrostatic pressures across the *Necturus* gallbladder. The curves are actual experimental tracings from x-y plot records of the steady-state interspace geometry of tissue bathed in chloride Ringer solution. Fig. 8 (right). Volume of lateral space in Fig. 7 plotted as a function of applied transepithelial hydrostatic pressure gradient. The ordinate is the volume of the interspace in cubic micrometers per micrometer of linear circumference of the cell at the level of the tight junction. The smooth curve is the characteristic compliance function for a thin-wall elastic tube (18) fitted to the data by the method of least squares. The equation for this curve is  $R = 1/1 + 1.13e^{-0.2\Delta P}$ ; correlation coefficient, .93.

(Fig. 6). The lateral intercellular spaces collapsed when fluid transport was inhibited by any of several different means (removal of mucosal sodium, replacement of  $\text{Cl}^-$  by  $\text{SO}_4^{2-}$ , or serosal ouabain). Restoration of transport caused rapid opening of the lateral spaces. The time course of these dimensional changes of the interspaces and the epithelial cells has been investigated (15).

Variation in the width of lateral intercellular spaces with hydrostatic pressure has been reported (16). To determine the compliance of the walls of the spaces, we studied the relationship between interspace shape and hydrostatic pressure difference across the gallbladder. The preparations were perfused with either 100 mM NaCl Ringer solution or 50 mM  $\text{Na}_2\text{SO}_4$  Ringer solution (13). An interspace that did not contain large dilations or irregular regions was selected for study and light output was recorded as a function of focal depth. As indicated in Fig. 2, this is readily accomplished by recording the focal depth as the  $x$ -axis of an  $x$ - $y$  plotter, and the phototube current as the  $y$ -axis. To achieve known hydrostatic pressure differences across the gallbladder, the fluid outflow tubes were occluded and the perfusion reservoirs elevated to the appropriate levels. The experimental tracings are shown in Fig. 7. The lateral space width was calculated from its linear relationship to phototube current at each pressure (17). It may be seen that space width increased if the serosal pressure exceeded the mucosal pressure by as little as 5  $\text{cm-H}_2\text{O}$ . The interspaces reached a maximum width at pressure differences of 10 to 15  $\text{cm-H}_2\text{O}$ . Records of phototube current versus focal depth over the cells adjacent to the space in Fig. 7 were similar to those shown in Fig. 4B; only small changes in cell density occurred as a function of pressure.

The volume of the lateral spaces per micrometer of linear circumferential length was calculated from the measurements of space width as a function of depth. Figure 8 shows the pressure-volume relationship for the space in Fig. 7. The relationship appeared to be sigmoidal, and the data were fitted by the method of least squares to the equation

$$R = \frac{1}{1 + \alpha e^{-\beta \Delta P}}$$

where  $R$  is the ratio of the volume of the interspace to its maximum volume,  $\alpha$  is a constant that determines the  $y$  intercept at zero pressure difference,  $\beta$  is the stiffness constant for the lateral cell membranes, and  $\Delta P$  is the hydrostatic pressure difference across the epithelium.

Table 1. Mean widths ( $\pm$  S.E.) of 23 lateral intercellular spaces of *Necturus* gallbladder epithelium at 2- $\mu\text{m}$  intervals of depth from the tight junction to the base of the cells.

Depth ( $\mu\text{m}$ )	Interspace width ( $\mu\text{m}$ )
0	0
2	$0.238 \pm 0.063$
4	$0.322 \pm 0.082$
6	$0.560 \pm 0.125$
8	$0.815 \pm 0.163$
10	$0.980 \pm 0.187$
12	$1.134 \pm 0.201$
14	$1.345 \pm 0.205$
16	$1.343 \pm 0.215$

This equation is an approximation to the pressure-volume characteristics of a thin-wall elastic tube (18). The line in Fig. 8 is the least-squares fit of this function to the data points. Six interspaces were analyzed at all six hydrostatic pressure differences with the tissue bathed in chloride Ringer solution. The parameter values (mean  $\pm$  S.E.) are  $\alpha = 2.4 \pm 1.1$ ,  $\beta = 0.25 \pm 0.03$  ( $\text{cm-H}_2\text{O}$ ) $^{-1}$ , and average correlation coefficient = .81. The distension of the lateral spaces on application of serosal pressure could be due either to filtration of serosal fluid into the spaces or to pressure-induced blockade of the exit of fluid transported by the cells. Since fluid transport by the cells could result in a pressure within the interspaces different from that in the bulk solution, the compliance curve was also determined in the absence of fluid transport—that is, with the gallbladder bathed in sulfate Ringer solution (19). The dilatation of the lateral spaces by changes in transepithelial hydrostatic pressure observed in sulfate Ringer solution must be due to filtration of serosal fluid across the basement membrane and connective tissue. For the lateral membranes of the cells in sulfate Ringer solution  $\beta = 0.38 \pm 0.05$  ( $\text{cm-H}_2\text{O}$ ) $^{-1}$ , ( $N = 5$ ),  $\alpha = 8.6 \pm 3.1$ , and average correlation coefficient = .97. These values indicate that the lateral intercellular spaces are highly compliant structures whose dimensions are dramatically changed by small hydrostatic pressure differences (20). A comparison of control interspace volume in chloride Ringer solution with the compliance curve measured in sulfate Ringer solution also allows an estimate of the transepithelial hydrostatic pressure equivalent to active fluid transport. The dilatation of the interspaces accompanying fluid transport in chloride Ringer solution is approximately equal to that produced by a transepithelial hydrostatic pressure gradient of 3.2  $\text{cm-H}_2\text{O}$  (serosa greater than mucosa).

It is apparent that in the absence of a

hydrostatic pressure difference, lateral intercellular spaces are clearly visible in *Necturus* gallbladder only during fluid transport, an observation in good agreement with previous electron microscopic evidence. The dilatation of the spaces in response to small hydrostatic pressure differences shows that alterations in lateral space morphology may be readily achieved by slight variations in transepithelial physical factors. Since such small transepithelial hydrostatic pressure differences have been shown to reverse net fluid flow (21), the link between epithelial fluid transport and the size of the lateral intercellular spaces is further strengthened.

KENNETH R. SPRING

ARVID HOPE

Laboratory of Kidney and Electrolyte Metabolism, National Heart, Lung, and Blood Institute, Bethesda, Maryland 20014

#### References and Notes

1. R. T. Whitlock and H. O. Wheeler, *J. Clin. Invest.* **43**, 2249 (1964); J. M. Diamond, *J. Gen. Physiol.* **48**, 15 (1964); J. M. Torney and J. M. Diamond, *ibid.* **50**, 2031 (1967); E. M. Wright, A. P. Smulders, J. M. Torney, *J. Membr. Biol.* **7**, 198 (1972).
2. A. E. Hill, *Proc. R. Soc. London Ser. B* **190**, 99 (1975).
3. O. Fredericksen and J. Rostgaard, *J. Cell Biol.* **61**, 830 (1974).
4. C. J. Benzel, G. Parsa, D. K. Hare, *Am. J. Physiol.* **271**, 570 (1969); A. B. Maunsbach, *J. Ultrastruct. Res.* **15**, 242 (1966).
5. The urinary bladder of the toad *Bufo marinus* has also been successfully mounted in the chamber. The cells may be clearly visualized and the electrical properties are in good agreement with published values.
6. H. H. Ussing and K. Zerahn, *Acta Physiol. Scand.* **23**, 110 (1951).
7. The chamber, first described by J. A. Dvorak and W. F. Stotler [*Exp. Cell Res.* **68**, 144 (1971)], is available commercially from Carl Zeiss, New York. We modified the commercial chamber considerably and will provide, on request, detailed design drawings of the new chamber.
8. The mica disks and cover glass are cemented together with Canada balsam and baked at 100°C until dry. The mucosal electrodes are made from 50- $\mu\text{m}$ -diameter, Teflon-coated silver wire (Cooner Wire Co., Chatsworth, Calif.). They are chloridized in 0.1M HCl, washed, and placed in the channel in the lower cover glass with Canada balsam. The mica-cover glass-electrode combination is made in advance and attached to the spacer with silicone (RTV 118, General Electric, Waterford, N.Y.). We found that this mucosal bath laminate did not need to be replaced unless it was damaged.
9. The microscope is equipped with an MPV-1 photometer (E. Leitz, Inc., Rockleigh, N.J.). The condenser is a 50  $\times$  0.6 numerical aperture (n.a.) objective lens designed for use as a condenser (model 620222), and the microscope objective lens is a 100  $\times$  1.3 n.a. oil-immersion lens (model 519249). Although the relatively narrow condenser aperture results in a modest reduction in the resolution of the optical system (from 0.2 to 0.3  $\mu\text{m}$ ), the contrast of the preparation is greatly enhanced. Sharp delineation of the boundaries of the lateral spaces is achieved and a well-corrected, highly reduced field-stop diaphragm is imaged over a relatively shallow depth of field. The preparation is illuminated by a circle of light 75  $\mu\text{m}$  in diameter; the image is viewed through the eyepieces only during the setup period (to prevent heating of the preparation the light intensity used is low, which makes it difficult to see much detail unless one is dark-adapted). The preparation is typically observed via closed circuit television by means of an image-intensified television camera (model 4410 SIT, Cohu Inc., San Diego, Calif.) attached to the viewing telescope of the beam splitter. In-

- accuracies in the microscope fine-focus adjustment result in an  $\sim 4$  percent error in measurements of focal depth.
10. E. Frömter, *J. Membr. Biol.* **8**, 259 (1972); L. Reuss and A. Finn, *ibid.* **25**, 115 (1975); C. H. Van Os and J. E. G. Slegers, *ibid.* **24**, 341 (1975).
  11. C. J. Bentzel, K. Loeschke, E. L. Benedetti, in *Proceedings of the International Union of Physiological Sciences, 27th International Congress (French National Committee of Physiological Sciences, Paris, 1977)*, vol. 13, p. 68.
  12. J. M. Diamond and W. H. Bossert, *J. Gen. Physiol.* **50**, 2061 (1967); L. A. Segel, *J. Theor. Biol.* **29**, 233 (1970); A. E. Hill, *Proc. R. Soc. London Ser. B* **190**, 115 (1975); J. J. Lim and J. Fischbarg, *Biochim. Biophys. Acta* **443**, 339 (1976); R. Huss and D. Marsh (18).
  13. The perfusion fluid composition is given in table 1 in K. R. Spring and G. Kimura, *J. Membr. Biol.* **38**, 233 (1978).
  14. Epithelial thickness is altered by the stretching of the gallbladder during mounting. In the experiments reported here, the tissue was tightly stretched to minimize movements during alterations in hydrostatic pressure. Minimal stretching results in a cell height of 32 to 36  $\mu\text{m}$ ; however, interspace shape and width are similar to those reported here.
  15. K. R. Spring and A. Hope, in preparation.
  16. C. L. Voute and H. H. Ussing, *J. Cell Biol.* **36**, 625 (1968); C. L. Voute, K. Møllgaard, H. H. Ussing, *J. Membr. Biol.* **21**, 273 (1975); C. L. Voute and H. H. Ussing, *Exp. Cell Res.* **62**, 375 (1970); C. J. Bentzel, *Kidney Int.* **2**, 324 (1972).
  17. The lateral space width was measured at one focal depth and the corresponding phototube current was recorded. The increase in phototube current over that measured at the level of the tight junction was divided by the measured space width (assuming zero width at the level of the junction). The slope of a plot of the change in current against the change in width was used to calculate the interspace width at the other focal depths. This calibration was repeated at each hydrostatic pressure difference. The width measurements are accurate within 0.15  $\mu\text{m}$ .
  18. R. Huss and D. Marsh, *J. Membr. Biol.* **23**, 305 (1975).
  19. K. Loeschke, G. M. Eisenbach, C. J. Bentzel, *Excerpta Med. Int. Congr. Ser. No. 391* (1975), p. 406; J. M. Diamond, *J. Physiol. (London)* **161**, 503 (1962).
  20. The basement membrane and connective tissue offer a finite hydraulic resistance, and the hydrostatic pressure within the lateral spaces will be slightly lower than that in the serosal medium. The amount of this pressure drop depends on the transepithelial volume flow induced by the hydrostatic pressure difference. Since the effective pressure gradient across the lateral membranes of the cells is actually less than that exerted transepithelially, the interspaces are probably even more compliant than our measurements indicate.
  21. R. I. Kiemowitz and T. L. Stanton, *Clin. Res.* **20**, 598 (1972); J. Fischbarg, C. R. Warshavsky, J. J. Lim, *Nature (London)* **266**, 71 (1977); C. H. Van Os and G. Wiedner, in *Proceedings of the International Union of Physiological Sciences, 27th International Congress (French National Committee of Physiological Sciences, Paris, 1977)*, vol. 13, p. 778.
  22. We were greatly helped in the design and fabrication of the chamber by J. Sullivan. The television equipment was put into operation with the assistance of W. Whitehouse, and the optical system was selected by M. Nahmmacher.

3 October 1977; revised 13 December 1977

## Separation of the Sperm Agglutinin and the Acrosome Reaction-Inducing Substance in Egg Jelly of Starfish

**Abstract.** *The egg jelly of the starfish Asterias amurensis was separated into the fractions J1, J2, and J3 on a Sephadex G-100 column. The J1 fraction induced the acrosome reaction and J2 induced sperm agglutination. Chemical analysis and chromatography revealed that sperm agglutinin is similar to asterosaponin A.*

In marine invertebrates, the egg jelly coat often shows physiological activity and plays an important role in fertilization. In sea urchins, egg jelly induces the acrosome reaction (1), sperm agglutination (2), and acceleration of sperm respiration (3). The first of these is an indispensable step for fertilization since the egg plasma membrane can fuse only with the membrane of the acrosomal process, which is newly formed during the acrosome reaction (4). However, the meaning, if any, of the phenomenon of sperm

agglutination is unknown. The fertilizin-antifertilizin theory (5) describes the agglutination reaction as a binding, like that of an immune reaction, between specific substances on the gamete surfaces. We think that the attachment of the sperm to the jelly surface initiates the interaction between the two gametes, and that sperm agglutination may reflect only this initial interaction.

Egg jelly consists mainly of glycoprotein. That of sea urchins contains sialic acid (6) and fucose sulfate (7) as the main

sugar components. Ishihara and Dan (8) have suggested the existence of fragments which induce the acrosome reaction but not sperm agglutination. A mucopolysaccharide-protein complex from starfish egg jelly has been obtained by phenol extraction (9). Which part of the egg jelly induces the acrosome reaction or sperm agglutination is still not known. Also it is not known whether sperm agglutinin and the acrosome reaction-inducing substance are identical to each other and what the chemical structure of the active substance is. We have succeeded in isolating the sperm agglutinin, free from the acrosome reaction-inducing substance, from the egg jelly of the starfish *Asterias amurensis*.

Suspensions of eggs, obtained by treating the ovaries with 1-methyladenine (10), were centrifuged at 6000g for 20 minutes, and the supernatant was used as the crude egg jelly. This was applied to a Sephadex G-100 column and separated into J1, J2, and J3 (Fig. 1a).

Spermatozoa, which had been washed with seawater containing 1 mM histidine, were diluted with 100 volumes of seawater. An equal volume of each fraction and a diluted sperm suspension were mixed and observed under microscopy. Only J1 induced the acrosome reaction and only J2 induced the sperm agglutination (Table 1 and Fig. 2). Fraction J3 also showed a weak agglutinating activity because of an overlap with J2, the sperm agglutinin; sperm agglutinin and the acrosome reaction-inducing substance are different from each other (Fig. 1). The sperm agglutination by jelly is irreversible in the starfish, whereas it is reversible in sea urchins. The agglutination caused by J2 was also irreversible.

The J1 fraction was separated on a Sepharose 4B column into subfractions consisting largely of (i) methylpentose-rich glycoproteins and (ii) hexose-rich glycoproteins.

The J2 fraction was undialyzable, but on Sephadex G-100 or G-50 it behaved as a small molecule; J2 has some affinity to Sephadex, a characteristic of many aromatic compounds. By ion-exchange column chromatography on DEAE-Sephadex A-25, J2 was separated into three fractions, one of which (2-2 in Fig. 1b) had agglutinating activity and contained a peptide moiety.

This sperm agglutinin was further purified by partition between *n*-butanol and 0.1M citrate buffer (pH 3.6). The agglutinating activity was recovered in the *n*-butanol layer. These two fractions were separated by thin-layer chromatography (TLC) on Kieselgel 60 (Merck) developed in a system consisting of chloro-

Fig. 1. (a) Elution profile of crude egg jelly from a Sephadex G-100 column. Abbreviations:  $V_0$ , void volume;  $V_t$ , total volume. (b) Elution profile of fraction J2 from a DEAE-Sephadex A-25 column eluted with a concave gradient from 0.5M pyridine, 0.25M acetic acid buffer (pH 5.2) to 1.0M pyridine, 0.5M acetic acid buffer (pH 5.2). (.....) Absorbance at 280 nm; (—) sugar content as determined by phenol-sulfuric acid methods.

